[including the $F(0)$ term calculated from the known chemical composition]. This represents ten parameters to be refined (eight phases $+K+\sigma$) from 27 observations. The initial estimate of $K_c$ was derived from

$$K_c = F(0)/\sum_{h'} F(h')^2. \qquad (23)$$

Equation (23) assumes that the $F(h')$ are on an absolute scale.

Table 1 summarizes the results of the refinement of random phases for ten consecutive trials. To obtain an additional figure of merit, the $R$ value was also computed at the end of each refinement cycle. The refinement process stopped when further minimization of $M$ produced no decrease of $R$. Inspection of Table 1 indicates that most trials (eight out of ten) converged in four-five cycles. Trial 5 has been selected to show the refinement process in more detail. Table 2 lists the results of the refinement, Fig. 2 illustrates the evolution of $M$ and $R$ as functions of the number of cycles and Fig. 1 reproduces the final Fourier map computed with the estimates of the structure factors obtained from (9).

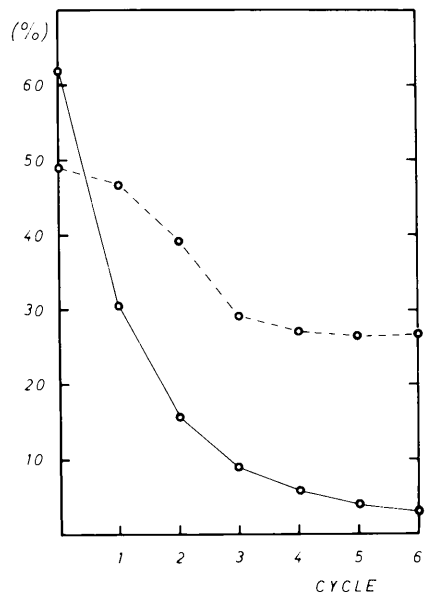


Fig. 2. $M$ (solid line) and $R$ (dashed line) as a function of the number of cycles of refinement for trial 5.

One of the authors (JR) thanks Eva Prats for her help. The financial support of the CSIC and DGICYT (Project PB89-0036) is gratefully acknowledged.

### References

DEBAERDEMAEKER, T., TATE, C. & WOOLFSON, M. M. (1985). *Acta Cryst.* A**41**, 286-290.
GERMAIN, G. & WOOLFSON, M. M. (1968). *Acta Cryst.* B**24**, 91-96.
HOPPE, W. (1963). *Z. Kristallogr.* **118**, 121-126.
JONES, N., MARSH, R. & RICHARDS, J. (1965). *Acta Cryst.* **19**, 330-336.
KARLE, J. & HAUPTMAN, H. (1956). *Acta Cryst.* **9**, 635-651.
KARLE, J. & KARLE, I. L. (1966). *Acta Cryst.* **21**, 849.
KRABBENDAM, H. & KROON, J. (1971). *Acta Cryst.* A**27**, 48-53.
PATTERSON, A. L. (1935). *Z. Kristallogr.* **90**, 517-542.
RIUS, J. & MIRAVITLLES, C. (1989). *Acta Cryst.* A**45**, 490-494.
ROLLET, J. S. (1970). In *Crystallographic Computing*, edited by F. R. AHMED, pp. 167-181. Copenhagen: Munksgaard.
ROLLET, J. S., MCKINLAY, T. G. & HAIGH, N. P. H. (1976). In *Crystallographic Computing*, edited by F. R. AHMED, pp. 413-419. Copenhagen: Munksgaard.
SAYRE, D. (1952). *Acta Cryst.* **5**, 60-67.
SAYRE, D. (1972). *Acta Cryst.* A**28**, 210-212.
SAYRE, D. (1974). *Acta Cryst.* A**30**, 180-184.
SCHENK, H. (1973). *Acta Cryst.* A**29**, 77-82.

*Acta Cryst.* (1991). A**47**, 571-577

## Resolution Functions of Powder Diffractometers at a Synchrotron-Radiation Source

BY T. WROBLEWSKI

*Hamburger Synchrotronstrahlungslabor HASYLAB, Deutsches Elektronen Synchrotron DESY, Hamburg, Germany*

(*Received* 22 *October* 1990; *accepted* 17 *April* 1991)

### Abstract

The resolution functions for various powder diffractometers using parallel-beam geometry are calculated. These diffractometers consist of monochromator, sample and eventually a post-specimen analyser. The theory is thus similar to that of two- or three-axis diffractometers. Special attention has to be given to the different diffraction mechanisms occurring at perfect crystals, synthetic multilayers or mosaic crystals. Resolution functions for all three types of monochromators are presented. Experiments performed at HASYLAB and other laboratories show good agreement with theory.

0108-7673/91/050571-07$03.00 

## Introduction

Synchrotron radiation exhibits an intense continuous spectrum and a high collimation. Powder diffraction experiments at a synchrotron-radiation source are thus mainly done in parallel-beam geometry. In the angular dispersive mode - the energy dispersive diffraction will not be treated in this paper - a monochromator selects a wavelength band out of the continuous spectrum. This monochromator is usually a perfect single crystal or a nondispersive double-crystal arrangement which can be a pair of single crystals (Wroblewski, Ihringer & Maichle, 1988) in the $(n, -n)$ setting or a channel-cut crystal (Cox, Hastings, Thomlinson & Prewitt, 1983; Parrish, Hart & Huang, 1986). Recently, synthetic multilayers (Stephenson, 1988; Wroblewski, Eichhorn, Ihringer, Kirfel & Lux, 1988) and mosaic crystals (Hohlwein, Siddons & Hastings, 1988; Wroblewski, 1990*a*) have also been applied. The radiation diffracted by the powder is analysed by a receiving slit, a position-sensitive detector or a Soller collimator or by a dispersive element like an analyser crystal.

The resolution function for neutron powder diffractometers, given by the Caglioti formula (Caglioti, Paoletti & Ricci, 1958; Caglioti, Paoletti & Ricci, 1960), applies only to one mosaic crystal as monochromator and a nondispersive detecting system (slit, position-sensitive detector, Soller slit). A more general approach was used by Bubakova, Drahokoupil & Fingerland (1961) for a triple-crystal diffractometer with mosaic and/or perfect crystals. Their approach can be generalized, treating the powder sample as a crystal with infinite mosaic spread. Although there have been several papers dealing with multicrystal arrangements (Cooper & Nathans, 1966; Nielsen & Bjerrum Moller, 1968; Pynn, Fujii & Shirane 1983; Cowley, 1987), there is to my knowledge only one author (Sabine, 1987) treating powder diffractometers. Although this author mentioned the 'Darwin solution' for perfect crystals he did not account for the differences between perfect crystals and mosaic crystals. For perfect crystals the incident and reflected rays always form the same angle with the reflecting lattice planes while for mosaic crystals the sum of both angles remains constant. Taking this into account mosaic and perfect crystals give different resolution functions.

In the following the approach of Bubakova, Drahokoupil & Fingerland (1961) will be used to determine the resolution functions of several powder diffractometers. After a general formulation for a multicrystal arrangement, several arrangements typical for powder diffractometry will be investigated. The resolution functions of powder diffractometers are then calculated in the Gaussian approximation and compared to experimental results.

## General theory

For a multicrystal arrangement the intensity at an angle $\gamma$ from the peak position is given by the convolution of the angular $H(\alpha, \varphi)$ and spectral $I_0(\lambda)$ distribution of the incident beam with the transmission functions $T_i$ of all following optical elements and the acceptance of the detector $S$.

$$I(\gamma) = \int \ldots \int \mathrm{d}\lambda\ \mathrm{d}\alpha\ \mathrm{d}\varphi\ \mathrm{d}\beta_1 \ldots \mathrm{d}\beta_n\ \mathrm{d}\varepsilon_1 \ldots \mathrm{d}\varepsilon_n \times I_0(\lambda)\ H(\alpha, \varphi) \prod_{i=1}^{n} T_i(\beta_i, x_i, y_i, \varepsilon_i) \times S(\gamma, x_n, \beta_n, \varepsilon_n). \quad (1)$$

At a synchrotron-radiation source $I_0(\lambda)$ is a slowly varying function and can be taken as constant. $H(\alpha, \varphi)$ can be decomposed into a component in the reflection plane, $F(\alpha)$, and another component perpendicular to it, $G(\varphi)$. The transmission function for the $i$th crystal $T_i$ can be written as a product of its Darwin width $D(x_i - y_i, \varepsilon_i)$ and the mosaic distribution $M(\beta_i, \varepsilon_i)$. $\beta_i$ is the in-plane deviation of a mosaic block of the $i$th crystal from the exact Bragg angle. $y_i = \Delta\lambda(\mathrm{d}\Theta_i/\mathrm{d}\lambda)$ describes the deviation from the Bragg condition due to the wavelength spread while $x_i$ gives the angular deviation from the Bragg position $\Theta_i$ at the $i$th crystal. $x_i$ is given by the misset $\beta_i$ of the $i$th crystal and the deviation in the direction of the incident beam which is due to the divergence and deviations caused by previous reflections and can be found recursively.

$$x_i = \sigma_{i-1,i}(x_{i-1} + \beta_{i-1}) + \beta_i \quad (2)$$

where $\sigma_{i-1,i}$ is $-1$ or $+1$ according to whether the crystals $i-1$ and $i$ are on the same $(-1)$ or on opposite sides $(+1)$ of the beam. For the first crystal $x_0 = 0$ and $\beta_0 = \alpha$, leading to $x_1 = \alpha + \beta_1$. $S(\gamma + x_n + \beta_n, \varepsilon_n)$ describes the entrance slit in front of the detector. If an open detector is used and if the scan is done with the last crystal the acceptance of the detector, $S$, is constant and $\beta_n$ in $T_n$ must be replaced by $\beta_n - \gamma$.

The $\varepsilon_i$ arise from the out-of-plane contributions of the divergence and the mosaic spreads. They can be calculated following Azaroff (1974). They are of second order and will therefore be neglected in the following. This is justified even for the infinite mosaicity of a powder because in the experiment only a small part of the Debye–Scherrer cone is detected, corresponding to a small out-of-plane mosaicity. With this assumption the integration over $\varphi$ and all $\varepsilon_i$ can be carried out and we obtain with $I_0(\lambda) = \text{constant}$

$$I(\gamma) \simeq \int \ldots \int \mathrm{d}\lambda\ \mathrm{d}\alpha\ \mathrm{d}\beta_1 \ldots \mathrm{d}\beta_n \times F(\alpha) \prod_{i=1}^{n} \{D_i(x_i - y_i) M_i(\beta_i)\} S(\gamma + x_n + \beta_n) \quad (3a)$$

or

$$I(\gamma) \simeq \int \ldots \int \mathrm{d}\lambda\ \mathrm{d}\alpha\ \mathrm{d}\beta_1 \ldots \mathrm{d}\beta_n \times F(\alpha) \prod_{i=1}^{n} \{D_i(x_i - y_i)\, M_i(\beta_i)\} \times D_n(x_n - y_n) M_n(\beta_n - \gamma). \quad (3b)$$

Equation (3*a*) is valid for a scan with a slit system in front of the detector, (3*b*) holds for an analyser crystal.

Equations (1) and (3) are valid for every type of multicrystal diffractometer. To apply it to powder diffractometers we will assume that one of the crystals has infinite mosaicity, which means $M(\beta)$ = constant. To separate instrumental effects from sample effects we will assume a vanishing Darwin width for the powder, $D(x-y) = \delta(x-y)$.

## Cases of practical interest

(*a*) *Perfect-crystal monochromator, slit in front of detector*

For a perfect-crystal monochromator $M_1(\beta_1) = \delta(\beta_1)$ leads to

$$I(\gamma) \simeq \iiint \mathrm{d}\lambda\ \mathrm{d}\alpha\ \mathrm{d}\beta_2 F(\alpha) D_1(\alpha - y_1) \times S(\gamma + \sigma_{1,2}\alpha + 2\beta_2) \quad (4)$$

using $y_i = \Delta\lambda(\mathrm{d}\Theta_i/\mathrm{d}\lambda) = \Delta\lambda \tan\Theta_i$ and $x_2 = \sigma_{1,2}\alpha + \beta_2 = y_2$ we can substitute $\Delta\lambda$ and carry out the integration over $\lambda$:

$$I(\gamma) \simeq \iint \mathrm{d}\alpha\ \mathrm{d}\beta_2\ F(\alpha) D_1\{\alpha(1 - \sigma_{1,2}\tan\Theta_1/\tan\Theta_2) - \beta_2(\tan\Theta_1/\tan\Theta_2)\} S\{\gamma + \sigma_{1,2}\alpha + 2\beta_2\}. \quad (5)$$

(*b*) *Perfect-crystal monochromator, perfect-crystal analyser*

In this case $M_1(\beta_1) = \delta(\beta_1)$ and $M_3(\beta_3 - \gamma) = \delta(\beta_3 - \gamma)$, leading to

$$I(\gamma) \simeq \iiint \mathrm{d}\lambda\ \mathrm{d}\alpha\ \mathrm{d}\beta_2 F(\alpha)\ D_1(\alpha - y_1) \times D_3[\gamma + \sigma_{2,3}(\sigma_{1,2}\alpha + 2\beta_2) - y_3]. \quad (6)$$

Again, we can replace $\Delta\lambda$ and carry out the integration over $\lambda$, yielding

$$I(\gamma) \simeq \iint \mathrm{d}\alpha\ \mathrm{d}\beta_2\ F(\alpha) D_1\{\alpha(1 - \sigma_{1,2}\tan\Theta_1/\tan\Theta_2) - \beta_2(\tan\Theta_1/\tan\Theta_2)\} \times D_3\{\gamma + \alpha\sigma_{1,2}(\sigma_{2,3} - \tan\Theta_3/\tan\Theta_2) + \beta_2(2\sigma_{2,3} - \tan\Theta_3/\tan\Theta_2)\}. \quad (7)$$

(*c*) *Mosaic-crystal monochromator, slit in front of detector*

For mosaic crystals the Darwin width is in most cases negligible compared to the mosaic spread. We can therefore set $D_1(x_1 - y_1) = \delta(x_1 - y_1)$. With $\beta_1 = y_1 - \alpha$ we get

$$I(\gamma) \simeq \iiint \mathrm{d}\lambda\ \mathrm{d}\alpha\ \mathrm{d}\beta_2 F(\alpha) M_1(y_1 - \alpha) \times S[\gamma + \sigma_{1,2}(2y_1 - \alpha) + 2\beta_2]. \quad (8)$$

Insertion of $\Delta\lambda$ gives

$$I(\gamma) \simeq \iint \mathrm{d}\alpha\ \mathrm{d}\beta_2\ F(\alpha)\ M_1\{\alpha(\sigma_{1,2}\tan\Theta_1 - \tan\Theta_2)/N + \beta_2\tan\Theta_1/N\} S\{\gamma - \alpha\sigma_{1,2}\tan\Theta_2/N + 2\beta_2(\tan\Theta_2 - \sigma_{1,2}\tan\Theta_1)/N\} \quad (9)$$

with $N = \tan\Theta_2 - 2\sigma_{1,2}\tan\Theta_1$.

(*d*) *Mosaic-crystal monochromator, perfect-crystal analyser*

Making the same assumptions as for cases (*b*) and (*c*) we get

$$I(\gamma) \simeq \iiint \mathrm{d}\lambda\ \mathrm{d}\alpha\ \mathrm{d}\beta_2\ F(\alpha) M_1(y_1 - \alpha) \times D_3\{\gamma + \sigma_{2,3}[\sigma_{1,2}(2y_1 - \alpha) + 2\beta_2] - y_3\}. \quad (10)$$

Replacing the $y_i$ and carrying out the integration over $\lambda$ we get

$$I(\gamma) \simeq \iint \mathrm{d}\alpha\ \mathrm{d}\beta_2 F(\alpha) M\{\alpha(\sigma_{1,2}\tan\Theta_1 - \tan\Theta_2)/N + \beta_2\tan\Theta_1/N\} \times D_3\{\gamma + \alpha\sigma_{1,2}(\tan\Theta_3 - \sigma_{2,3}\tan\Theta_2)/N + \beta_2(2\sigma_{2,3}\tan\Theta_2 - 2\sigma_{1,2}\sigma_{2,3}\tan\Theta_1 - \tan\Theta_3)/N\}. \quad (11)$$

(*e*) *Double-crystal monochromators*

For a double-crystal monochromator with two identical perfect crystals in the (+, −) setting or the equivalent case of a channel-cut crystal, $D_1$ would have to be replaced by $D_1 * D_2$ and all the following indices incremented by 1. But since $D_1$ and $D_2$ are identical $D_1^2$ can be used instead.

In the case of two mosaic crystals in the (+, −) setting we have $y_1 = y_2$. For vanishing Darwin widths we get $\beta_1 = -\beta_2$ so that the contributions of $\beta_1$ and $\beta_2$ to the $x_i$ ($i \geq 3$) cancel out. With $\beta_1 = y_1 - \alpha$ and a symmetric mosaic distribution we have the same expression as in the case of perfect crystals but with $D_1^2$ replaced by $M_1^2$.

(*f*) *Mosaic-crystal analyser*

If a mosaic crystal is applied as analyser crystal we have to replace $D_3(x_3 - y_3)$ by $M_3(\beta_3)$. Condition $x_3 = y_3$ gives $\beta_3 = y_3 - \sigma_{2,3}[\sigma_{1,2}(2y_1 - \alpha) + 2\beta_2]$ so that $M_3$ has the same form as $D_3$ and the same formalism can be applied.

### Gaussian approximation

The expressions calculated above can be evaluated numerically and will give not only the half width but also the peak shape. This will be treated in a forthcoming paper. A good estimate for the half width as a function of the diffraction angle at the powder sample can be obtained from a Gaussian approximation which allows an analytical solution of the above equations.

All the above integrals have the same form:

$$I(\gamma) \simeq \iint \mathrm{d}\alpha\ \mathrm{d}\beta_2\ F(\alpha) T_1(\alpha u_1 + \beta_2 v_1) \times T_3(\gamma + \alpha u_3 + \beta_2 v_3) \quad (12)$$

where $T$ now stands for $D$, $M$ or $S$ and the $u_i$ and $v_i$ are functions of the diffraction angles. In the Gaussian approximation we have

$$I(\gamma) \simeq \iint \mathrm{d}\alpha\ \mathrm{d}\beta_2 \exp(-\alpha^2/2\psi'^2) \times \exp\{-(\alpha u_1 + \beta_2 v_1)^2/2\Delta_1'^2\} \times \exp\{-(\gamma + \alpha u_3 + \beta_2 v_3)^2/2\Delta_3'^2\} \quad (13)$$

where $\psi'$ is given by the divergence of the incident beam and $\Delta_1'$ and $\Delta_3'$ are related to the Darwin width, the mosaic spread or the slit width. Integration over $\alpha$ and $\beta_2$ yields

$$I(\gamma) \simeq \exp\{-\gamma^2 v_1^2/2[v_1^2 \Delta_3'^2 + v_3^2 \Delta_1'^2 + (v_1 u_3 - v_3 u_1)^2 \psi'^2]\} \quad (14)$$

leading to an instrumental width $w'$,

$$w'^2 = \Delta_3'^2 + (v_3/v_1)^2 \Delta_1'^2 + \{(v_1 u_3 - v_3 u_1)/v_1\}^2 \psi'^2. \quad (15)$$

$w'$, $\Delta_1'$, $\Delta_3'$ and $\psi'$ are the $\sigma$ widths of the corresponding Gaussian curve. The half widths (FWHM) $w$, $\Delta_1$, $\Delta_3$ and $\psi$ can be obtained dividing each by $2\sqrt{\ln 2}$.

For the different cases treated above we get

$$(a)\quad w^2 = \Delta_3^2 + (2\tan\Theta_2/\tan\Theta_1)^2 \Delta_1^2 + \{(2\tan\Theta_2 - \sigma_{1,2}\tan\Theta_1)/\tan\Theta_1\}^2 \psi^2 \quad (16)$$

$$(b)\quad w^2 = \Delta_3^2 + \{(\tan\Theta_3 - 2\sigma_{2,3}\tan\Theta_2)/\tan\Theta_1\}^2 \Delta_1^2 + \{(2\sigma_{2,3}\tan\Theta_2 - \sigma_{2,3}\sigma_{1,2}\tan\Theta_1 - \tan\Theta_3)/\tan\Theta_1\}^2 \psi^2 \quad (17)$$

$$(c)\quad w^2 = \Delta_3^2 + \{2(\tan\Theta_2 - \sigma_{1,2}\tan\Theta_1)/\tan\Theta_1\}^2 \Delta_1^2 + \{(2\tan\Theta_2 - \sigma_{1,2}\tan\Theta_1)/\tan\Theta_1\}^2 \psi^2 \quad (18)$$

$$(d)\quad w^2 = \Delta_3^2 + \{(2\sigma_{2,3}\tan\Theta_2 - 2\sigma_{2,3}\sigma_{1,2}\tan\Theta_1 - \tan\Theta_3)/\tan\Theta_1\}^2 \Delta_1^2 + \{(2\sigma_{2,3}\tan\Theta_2 - \sigma_{2,3}\sigma_{1,2}\tan\Theta_1 - \tan\Theta_3)/\tan\Theta_1\}^2 \psi^2. \quad (19)$$

### Focusing

Most of the dispersive terms in the above expressions vanish for a certain angle $\Theta_2$. The occurrence of such a focusing point can be explained by simple arguments and can help to check the above expressions. As an example let us take the term proportional to the reflection width of the monochromator $\Delta_1$ for the case (*b*).

An ideal crystal does not produce additional divergence so that in the case of an incident parallel white beam a parallel beam with a certain bandwidth is reflected onto the sample. Here the Bragg condition gives $\Delta\lambda/\lambda = \beta_2 \cot\Theta_2$. The angular deviation caused by a grain tilted by $\beta_2$ is $2\beta_2$. To fulfil the condition $\Delta\lambda/\lambda = 2\beta_2 \cot\Theta_3$ for all $\lambda$ and $\beta_2$ we must have $2\tan\Theta_2 = \tan\Theta_3$. Otherwise different wavelengths are reflected at different angles.

From the above equations it is also clear that it is desirable to use not the dispersive ($\sigma_{i-1,i} = -1$) but the slightly dispersive ($n, -m$) setting ($\sigma_{i-1,i} = 1$), because the half width is generally smaller in this case.

### Comparison with experiments

To my knowledge only experiments using either one perfect crystal (or synthetic multilayer) or a double-crystal monochromator have been reported so far. Thus, only the resolution functions (*a*) and (*b*) can be compared with experimental values. Most experiments were performed by the author at HASYLAB beamline F1 (Wroblewski, Ihringer & Maichle, 1988), but also data from experiments at other beamlines in various laboratories [Cernik, Murray, Pattison & Fitch (1990) (Fig. 1); Küster, Limper & Reinhardt (1988) (Fig. 4); Cox, Hastings, Thomlinson & Prewitt (1983) (Fig. 5)] are compared with theory. Figs. 1 and 2 show resolution curves obtained with a receiving slit (or a Soller collimator). The resolution function for this case is given by (16). The mono-

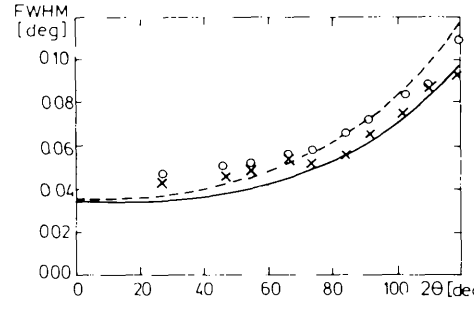


Fig. 1. Resolution functions for a channel-cut monochromator and a Soller slit in front of the detector. The monochromator was either Si(111) (full line, crosses) or Ge(111) (dashed line, circles). $\Delta_{1,\mathrm{Si}} = 6'' = 0{\cdot}029$ mrad, $\Delta_{1,\mathrm{Ge}} = 15'' = 0{\cdot}073$ mrad, $\Theta_{1,\mathrm{Si}} = 13{\cdot}83°$, $\Theta_{1,\mathrm{Ge}} = 13{\cdot}26°$, $\Delta_3 = 0{\cdot}56$ mrad, $\psi = 0{\cdot}12$ mrad, $\gamma = 0{\cdot}149855$ nm, sample: Si SRM640b. (Experimental values from Cernik, Murray, Pattison & Fitch, 1990.)

chromators were a channel-cut crystal (Fig. 1) or a synthetic multilayer (Fig. 2). Figs. 3–8 show the resolution for the case that a (perfect) analyser crystal is applied in front of the detector. In this case the resolution function is given by (17). The monochromators were a double perfect-crystal monochromator (Figs. 3–5), a synthetic multilayer (Fig. 6) and a double mosaic-crystal monochromator (Figs. 7, 8). In contrast to Fig. 3, the measurements of Fig. 4 were made at HASYLAB beamline B2 (Arnold *et al.*, 1989) with a focusing mirror in front of the monochromator which leads to a higher divergence $\psi$. The experimental values in Fig. 5 were taken from

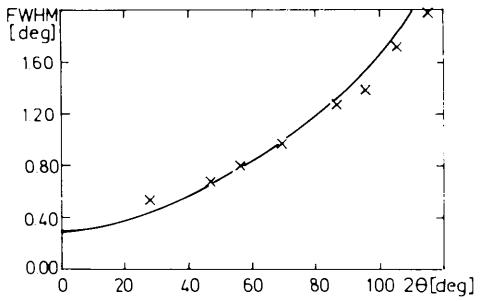


Fig. 2. Resolution function for a synthetic multilayer and a slit in front of the detector. $\Delta_1 = 90'' = 0{\cdot}44$ mrad, $\Theta_1 = 2{\cdot}15°$, $\Delta_3 = 5$ mrad, $\psi = 0{\cdot}1$ mrad, $\lambda = 0{\cdot}154$ nm, sample: Ge.

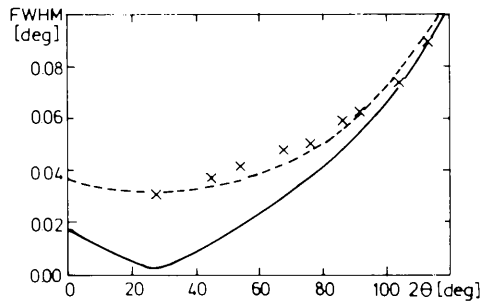


Fig. 3. Resolution function for an Si(111) double perfect-crystal monochromator and a perfect Si(111) analyser crystal in front of the detector. $\Delta_1 = \Delta_3 = 6'' = 0{\cdot}029$ mrad, $\Theta_1 = \Theta_3 = 14{\cdot}2°$, $\psi = 0{\cdot}15$ mrad, $\lambda = 0{\cdot}154$ nm, sample: Si SRM 640b. The deviation of the measured values (crosses) from theory (full line) can be explained by assuming a sample-dependent broadening of 0·03° (dotted line) probably caused by pressing the sample into the holder.

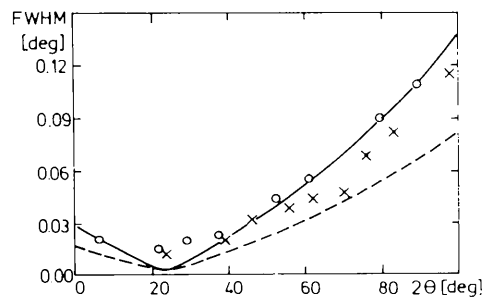


Fig. 4. Resolution function for an Si(111) double perfect-crystal monochromator and a perfect Si(111) analyser crystal in front of the detector. In contrast to Fig. 3 a focusing mirror was applied in front of the monochromator, leading to a higher divergence of the incident beam. $\Delta_1 = \Delta_3 = 5'' = 0{\cdot}024$ mrad, $\Theta_1 = \Theta_3 = 11{\cdot}78°$, $\psi = 0{\cdot}25$ mrad, $\lambda = 0{\cdot}128$ nm, samples: Si SRM 640b (crosses), mica (circles). The effect of the increased divergence (full line) on the resolution is evident. The dashed line shows the resolution function for an unfocused beam ($\psi = 0{\cdot}15$ mrad). (Experimental values from Küster, Limper & Reinhardt, 1988.)

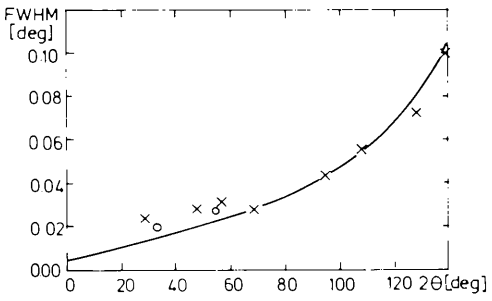


Fig. 5. Resolution function for an Si(220) double perfect-crystal monochromator in dispersive setting and a perfect Si(111) analyser. $\Delta_1 = 6'' = 0{\cdot}029$ mrad, $\Theta_1 = 23{\cdot}6°$, $\Delta_3 = 6'' = 0{\cdot}029$ mrad, $\Theta_3 = 14{\cdot}2°$, $\psi = 0{\cdot}14$ mrad, $\lambda = 0{\cdot}154$ nm, samples: $CeO_2$ (crosses), $Bi_2O_3$ (circles). (Experimental values from Cox, Hastings, Thomlinson & Prewitt, 1983.)

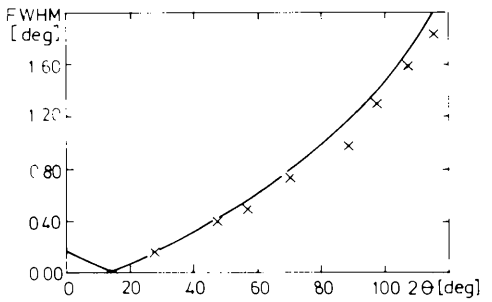


Fig. 6. Resolution function for a synthetic multilayer monochromator and an Si(111) analyser in front of the detector. $\Delta_1 = 90'' = 0{\cdot}44$ mrad, $\Theta_1 = 2{\cdot}15°$, $\Delta_3 = 6'' = 0{\cdot}029$ mrad, $\Theta_3 = 14{\cdot}2°$, $\psi = 0{\cdot}1$ mrad, $\lambda = 0{\cdot}154$ nm, sample: Ge.

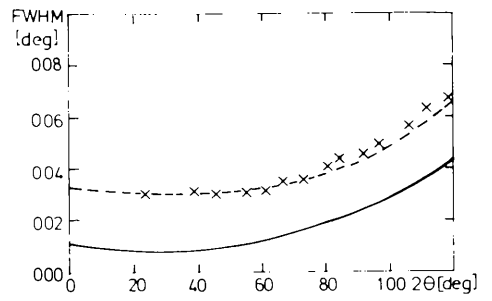


Fig. 7. Resolution function for a Be(004) double mosaic-crystal monochromator and an Si(111) analyser. $\Delta_1 = 45'' = 0{\cdot}22$ mrad, $\Theta_1 = 45°$, $\Delta_3 = 5'' = 0{\cdot}024$ mrad, $\Theta_3 = 11{\cdot}59°$, $\psi = 0{\cdot}15$ mrad, $\lambda = 0{\cdot}126$ nm. The sample was the same as in Fig. 3 so that the same corrections can be applied.

Cox, Hastings, Thomlinson & Prewitt (1983) who used a dispersive setting between monochromator and sample. All other measurements were made in the slightly dispersive setting. In all cases the variation of the half width with $2\Theta_2$ is well described.

Some of the measurements at the focused beamline B2 show, however, a halfwidth that is significantly smaller than the theoretical value. This can be explained by an asymmetric intensity distribution produced by the mirror. At grazing incidence an initial plane of radiation is output as an arc. In order to reach the focus an extreme ray must acquire an angle $\alpha_M$ given by (Heald & Hastings, 1981)

$$\alpha_M = 2\omega\varphi^2/(8\omega^2+\varphi^2) \qquad (20)$$

where $\omega$ is the glancing angle of the mirror (7 mrad) and $\varphi$ the horizontal divergence of the beam (4 mrad). This leads to a rather asymmetric intensity distribution which makes the Gaussian approximation inadequate. Recent numerical calculations for beamline B2 in which Darwin curves were used for $D_1$ and $D_3$ and $F(\alpha)$ was calculated using the ray-tracing program *SHADOW* (Lai & Cerrina, 1986) gave non-Gaussian profiles. Furthermore, peak shape and peak width are very sensitive to the mirror adjustment (Wroblewski, 1990*b*). Investigations of these effects are in progress and will be treated in a forthcoming paper.

## Future prospects

In all of the above resolution functions the dispersive terms contain the factor $1/\tan\Theta_1$. It is therefore desirable to go to high monochromator angles. Use of higher-order reflections of perfect monochromator crystals entails a dramatic decrease in intensity because of the decreasing Darwin widths. For a mosaic crystal, however, the reflection width is given by the mosaic spread and is therefore not angular dependent.

If the mosaic spread exceeds the angular divergence of the source a double-crystal arrangement performs better than a single-crystal monochromator because the peak width away from the focusing point cannot be pushed below (twice) the mosaic spread in the latter case.

While the term depending on $\Delta_1$ can be decreased by increasing $\tan\Theta_1$, the term depending on $\psi$ cannot be much smaller than $\psi$, except close to the focusing point.

Following these arguments the resolution function for a double mosaic-crystal monochromator at $\Theta_1 = 89°$ has been calculated. To have realistic values the parameters from beryllium crystals which have already been used successfully (Wroblewski, 1990*a*) have been chosen. The result can be seen in Fig. 9.

Another representation is given in Fig. 10. Here the resolution is expressed in $\Delta d/d$ as a function of $(\sin\Theta)/\lambda = 1/(2d)$. To allow a comparison, the resolution given by a perfect Si(111) monochromator is also shown. It has a minimum in a region where most

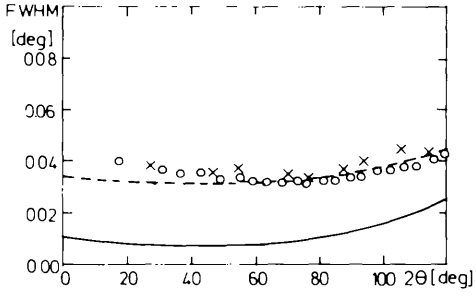


Fig. 8. Resolution functions for a Be(004) and a Be(006) monochromator. The reflections occur simultaneously. The wavelength can be selected by setting the analyser crystal to the desired angle. $\Delta_1 = 45'' = 0{\cdot}22$ mrad, $\Theta_1 = 60°$, $\Delta_3(\lambda_1) = 6'' = 0{\cdot}029$ mrad, $\Delta_3(\lambda_2) = 4'' = 0{\cdot}019$ mrad, $\Theta_3(\lambda_1) = 14{\cdot}2°$, $\Theta_3(\lambda_2) = 9{\cdot}45°$, $\psi = 0{\cdot}15$ mrad, $\lambda_1 = 0{\cdot}154$ nm, $\lambda_2 = 0{\cdot}103$ nm. The difference in the theoretical resolution (full line) for the two reflections cannot be resolved in this figure. As in Figs. 3 and 6, a broadening of 0·03° due to the sample has to be introduced. The crosses correspond to measurements at $\lambda_1$, the circles to the measurements at $\lambda_2$.

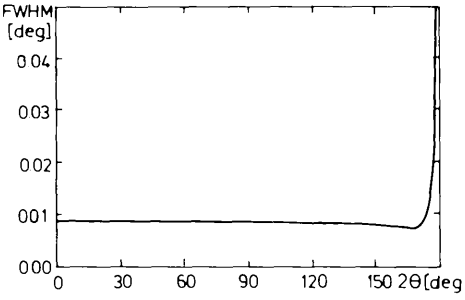


Fig. 9. Resolution function for a Be(006) double mosaic-crystal monochromator close to backscattering and an Si(111) analyser crystal (equation 17). $\Delta_1 = 45'' = 0{\cdot}22$ mrad, $\Theta_1 = 89°$, $\Delta_3 = 5'' = 0{\cdot}024$ mrad, $\Theta_3 = 10{\cdot}94°$, $\psi = 0{\cdot}15$ mrad, $\lambda = 0{\cdot}119$ nm.

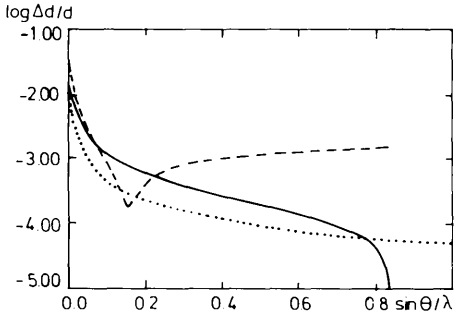


Fig. 10. Resolution functions in units of $\Delta d/d$ over $(\sin\Theta_2)/\lambda$. The full curve was obtained using the same parameters as for Fig. 9. The dashed curve gives the resolution for the case that Si(111) crystals are used at the same wavelength of 0·119 nm. The dotted line shows the limit that is given by the particle-size broadening arising from particles of 1 μm thickness.

substances have only few reflections, while at lower $d$ values, where the density of peaks is higher, the proposed arrangement shows a much better resolution. The superior performance of the mosaic-crystal monochromator becomes even more evident if the resolution functions are compared to the limit that is set by the particle-size broadening from the sample. $\Delta d/d$ cannot exceed the value given by $d/D$ where $D$ is the thickness of the particle. In Fig. 10 a particle thickness of 1 $\mu$m was chosen. While the curve for the mosaic monochromator comes close to this limit the curves for the conventional optics and that of the particle-size limit diverge. The performance of the perfect-crystal monochromator is only better in the focusing minimum where it goes even below the particle-size limit.

Taking coarser grains is no real solution since then they could in principle be better investigated by single-crystal diffraction at a synchrotron-radiation source (Bachmann, Kohler, Schulz & Weber, 1985), avoiding overlapping reflections.

## Concluding remarks

The resolution functions for different types of angle dispersive powder diffractometers in parallel-beam geometry have been calculated and compared with experimental values. It is shown that perfect-crystal monochromators at a low Bragg angle are not ideally suited to very high-resolution work although their performance is superior to diffractometers at conventional sources using focusing geometry. Therefore, a new arrangement employing mosaic crystals at angles close to backscattering is proposed, giving a resolution function close to the limit set by the particle-size broadening. Such an instrument would give the highest possible resolution that can be obtained with a polycrystalline sample.

## References


ARNOLD, H., BARTL, H., FUESS, H., IHRINGER, J., KOSTEN, K., LÖCHNER, U., PENNARTZ, P. U., PRANDL, W. & WROBLEWSKI, T. (1989). *Rev. Sci. Instrum.* **60**, 2380-2381.

AZAROFF, L. V. (1974). *X-ray Spectroscopy*. New York: McGraw-Hill.

BACHMANN, F., KOHLER, H., SCHULZ, H. & WEBER, H. P. (1985). *Acta Cryst.* A**41**, 35-40.

BUBAKOVA, R., DRAHOKOUPIL, J. & FINGERLAND, A. (1961). *Czech. J. Phys.* B**11**, 205-222.

CAGLIOTI, G., PAOLETTI, A. & RICCI, F. P. (1958). *Nucl. Instrum. Methods*, **3**, 223-228.

CAGLIOTI, G., PAOLETTI, A. & RICCI, F. P. (1960). *Nucl. Instrum. Methods*, **9**, 195-198.

CERNIK, R. J., MURRAY, P. K., PATTISON, P. & FITCH, A. N. (1990). *J. Appl. Cryst.* **23**, 292-296.

COOPER, M. J. & NATHANS, R. (1966). *Acta Cryst.* **23**, 357-367.

COWLEY, R. A. (1987). *Acta Cryst.* A**43**, 825-836.

COX, D. E., HASTINGS, J. B., THOMLINSON, W. & PREWITT, C. T. (1983). *Nucl. Instrum. Methods*, **208**, 573-578.

HEALD, S. M. & HASTINGS, J. B. (1981). *Nucl. Instrum. Methods*, **187**, 533-561.

HOHLWEIN, D., SIDDONS, D. P. & HASTINGS, J. B. (1988). *J. Appl. Cryst.* **21**, 911-915.

KÜSTER, A., LIMPER, W. & REINHARDT, J. (1988). HASYLAB Jahresbericht 1988, pp. 291-292. DESY, Hamburg, Germany.

LAI, B. & CERRINA, F. (1986). *Nucl. Instrum. Methods*, A**246**, 337-341.

NIELSEN, M. & BJERRUM MOLLER, H. (1968). *Acta Cryst.* A**25**, 547-550.

PARRISH, W., HART, M. & HUANG, T. C. (1986). *J. Appl. Cryst.* **19**, 92-100.

PYNN, R., FUJII, Y. & SHIRANE, G. (1983). *Acta Cryst.* A**39**, 38-46.

SABINE, T. M. (1987). *J. Appl. Cryst.* **20**, 23-27, 173-178.

STEPHENSON, G. B. (1988). *Nucl. Instrum. Methods*, A**266**, 447-451.

WROBLEWSKI, T. (1990*a*). *Proc. 2nd European Conf. on Progress in X-ray Synchrotron Radiaton Research*, edited by A. BALERNA, E. BERNIERI & S. MOBILIO, Vol. 25, pp. 319-325. Bologna SIF.

WROBLEWSKI, T. (1990*b*). HASYLAB Jahresbericht 1990, pp. 569-570. DESY, Hamburg, Germany.

WROBLEWSKI, T., EICHHORN, K., IHRINGER, J., KIRFEL, A. & LUX, B. (1988). *Z. Kristallogr.* **185**, 684.

WROBLEWSKI, T., IHRINGER, J. & MAICHLE, J. (1988). *Nucl. Instrum. Methods*, A**266**, 664-667.


*Acta Cryst.* (1991). A**47**, 577-590

# Which Symmetry Will an Ideal Quasicrystal Admit?

BY A. JANNER

*Institute for Theoretical Physics, University of Nijmegen, Toernooiveld, 6525 ED Nijmegen, The Netherlands*

(*Received* 14 *November* 1990; *accepted* 17 *April* 1991)

*A tribute in honour of Mrs C. H. MacGillavry**


## Abstract

The crystallographic nature of a quasicrystal structure is expressed in terms of the possibility of labeling 'translationally' equivalent atomic positions by a set of $n$ integers. The corresponding position vectors are integral linear combinations of $n$ basic ones generating a vector module $M$ of rank $n$ and dimension $m$. Because of the aperiodic nature of the quasicrystal, $n$ is larger than $m$. Typical values observed in nature


* Contribution based on a lecture delivered 8 December 1989 at the C. H. MacGillavry Symposium, Amsterdam.

0108-7673/91/050577-14$03.00